

# The dynamic model of a four control moment gyroscope system

## Modelo dinámico de un sistema de control de par por cuatro giróscopos

Eugenio Yime-Rodríguez <sup>a</sup>, César Augusto Peña-Cortés <sup>b</sup> & William Mauricio Rojas-Contreras <sup>c</sup>

<sup>a</sup> Facultad de Ingenierías, Universidad Tecnológica de Bolívar, Colombia. [eyime@unitecnologica.edu.co](mailto:eyime@unitecnologica.edu.co)

<sup>b</sup> Facultad de Ingenierías y Arquitecturas, Universidad de Pamplona, Colombia. [cesarapc@unipamplona.edu.co](mailto:cesarapc@unipamplona.edu.co)

<sup>c</sup> Facultad de Ingenierías y Arquitecturas, Universidad de Pamplona, Colombia. [mrojas@unipamplona.edu.co](mailto:mrojas@unipamplona.edu.co)

Received: November 28th, 2012. Received in revised form: February 20th, 2014. Accepted: May 9th, 2014.

### Abstract

The dynamic model of a Four Control Moment Gyroscope (4-CMG) is traditionally obtained after computing the derivative of the angular momentum equation. Although this approach leads to a simple dynamic model, new models have been introduced due to terms not taken into account during the computation of the angular momentum equation. In this paper, a new dynamic model for a 4-CMG based on the Newton-Euler algorithm, which is well accepted in Robotics, was developed. This new approach produces a complete dynamic model.

*Keywords:* dynamics, gyroscope, model; control.

### Resumen

El modelo dinámico de un sistema de control de par utilizando cuatro giróscopos (4-CMG) tradicionalmente se obtiene al calcular la derivada de la ecuación del momento angular total. Aunque este enfoque conduce a un modelo dinámico relativamente simple, recientemente se han introducido nuevos modelos debido a términos que no se han tenido en cuenta, o se desprecian, durante el cálculo de la ecuación del momento angular. En este artículo, se propone un nuevo modelo dinámico para un 4-CMG basado en el algoritmo de Newton-Euler, el cual es bien aceptado en robótica. Con este nuevo enfoque se logra obtener un modelo dinámico bastante completo.

*Palabras clave:* dinámica; giróscopo; modelo; control.

## 1. Introduction

A Four Control Moment Gyroscope (4-CMG) is an angular momentum exchange device used on satellites [1-3], submarines [4, 5], to control attitude. It is composed by four gyroscopes arranged in a pyramidal form, see Fig. 1, with the torque amplification property being its principal advantage [6]. Moreover, when used in satellites no fuel or gas propellant is required, because the motors use electricity to operate.

The dynamic model of a 4-CMG is usually obtained by differentiation of the angular momentum equation [7]. This is done in [3, 4] and [8]. Probably the most exact dynamic model using this approach is the developed by Ford and Hall, [8].

The first comparison between a robot arm and a 4-CMG was performed by Bedrossian et al. [9]; in this work an analogy of velocities was considered to study the singularities on a 4-CMG. No further analogies with robot arms were stated.

In this paper a kinematics comparison between a 4-CMG and a robotic arm is used to develop a new dynamic model. The advantages of this approach are: use of a widely accepted methodology to compute a dynamic model, and more precise equations.

## 2. Dynamic equations for A CMG

Fig. 1 illustrates a CMG with four gyroscopes, each of them composed of a flywheel and a gimbal. A coordinate frame  $\mathbf{x}_i, \mathbf{y}_i, \mathbf{z}_i$ , is located at the center of the flywheel, which serves as a reference for the motion of gimbals and flywheels. The flywheels turn at a constant speed, while the gimbals can rotate around  $\mathbf{y}_i$  axis without any restriction. The angle of rotation of a  $i$ -th gimbal is represented by  $\theta_i$ , with the zero position being illustrated in the figure. The position of the four gyroscopes is denoted by the vector  $\boldsymbol{\theta} = [\theta_1, \theta_2, \theta_3, \theta_4]^T$ . The angle  $\beta$  is the pyramid's skew angle.

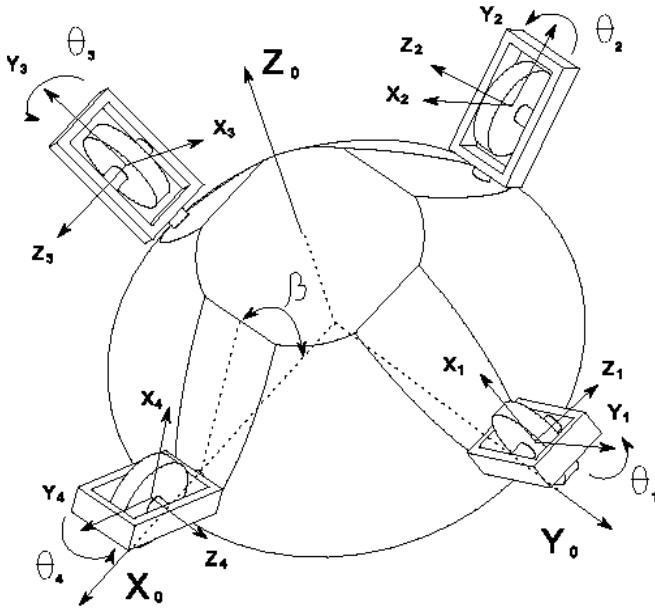


Figure 1. Control moment gyroscope with pyramidal array.

Fig. 2 illustrates the equivalent open kinematics chain for a 4-CMG; there the circles represent rotational joints.

To compute the dynamic model, two steps are performed, see Fig. 3. The first step is the Newton-Euler algorithm for each gyroscope, this led to the reaction forces and moments applied to the base body. The second step is the dynamic equation for the base body, where the reaction forces and moments exerted by each gyroscope,  $M_i$  and  $F_i$ , are involved. The angular and linear velocity of the base body,  $v_0$  and  $\omega_0$  respectively, plus the angular velocities of each joint,  $\omega_{i,1}$  and  $\omega_{i,2}$  are required in the Newton-Euler algorithm to perform the direct kinematics of the gyroscopes [10, 11].

Computation of the Newton Euler Equations for a serial robot is also done using two steps, Tsai [12]. The first one is the kinematics calculus toward the extreme of the robot, as shown in Table 1.

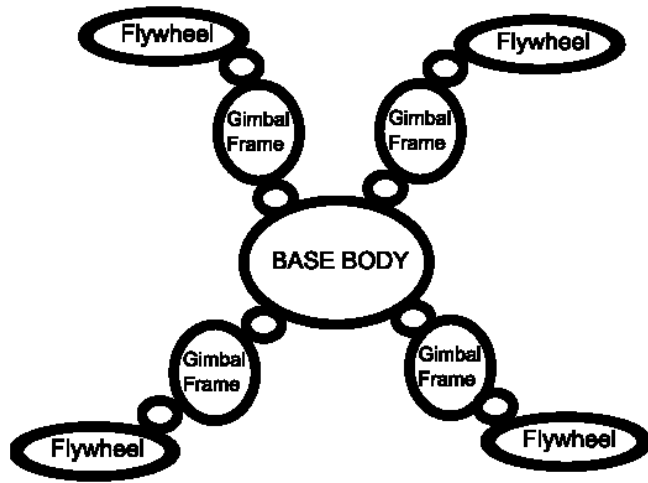


Figure 2. Equivalent kinematic chain of a 4-CMG.

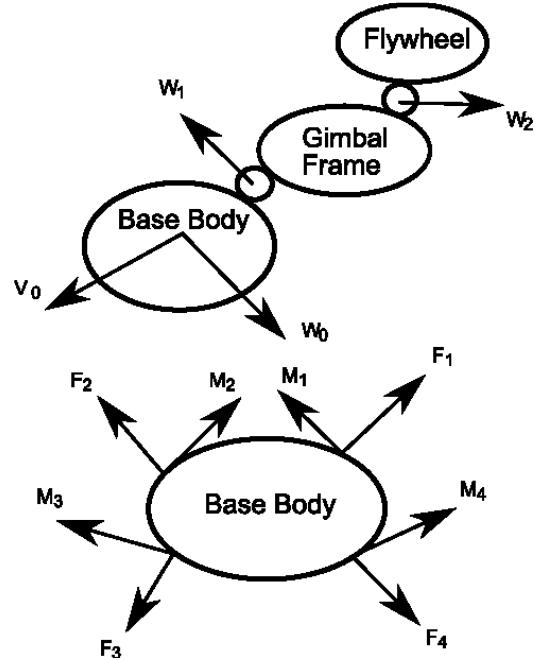


Figure 3. Gyroscope kinematics and Base body dynamics.

Table 1. Recursive Newton-Euler formulation. Forward kinematics.

Forward kinematics	
Angular velocity propagation	
${}^iR_i = \begin{bmatrix} \cos(\theta_i) & \sin(\theta_i) & 0 \\ -\cos(\alpha_i)\sin(\theta_i) & \cos(\alpha_i)\cos(\theta_i) & \sin(\alpha_i) \\ \sin(\alpha_i)\sin(\theta_i) & -\sin(\alpha_i)\cos(\theta_i) & \cos(\alpha_i) \end{bmatrix}$	
${}^{i-1}Z_{i-1} = [0 \ 0 \ 1]^T$	
Angular acceleration propagation	
$\dot{\omega}_i = \dot{\omega}_{i-1} + Z_{i-1}\ddot{\theta}_i + \omega_{i-1} + Z_{i-1}\dot{\theta}_i$	
${}^i\dot{\omega}_i = {}^iR_{i-1}({}^{i-1}\dot{\omega}_{i-1} + {}^{i-1}Z_{i-1}\dot{\theta}_i + {}^{i-1}\omega_{i-1} + {}^{i-1}Z_{i-1}\dot{\theta}_i)$	
Linear velocity propagation	
$v_i = v_{i-1} + \omega_i \times r_i$	
${}^i v_i = {}^iR_{i-1}({}^{i-1}v_{i-1} + {}^i\omega_i \times {}^i r_i)$	
${}^i r_i = [a_i \ d_i \sin(\alpha_i) \ d_i \cos(\alpha_i)]^T$	
Linear acceleration propagation	
$\dot{v}_i = \dot{v}_{i-1} + \dot{\omega}_i \times r_i + \omega_i \times (\omega_i \times r_i)$	
${}^i \dot{v}_i = {}^iR_{i-1}({}^{i-1}\dot{v}_{i-1} + {}^i\dot{\omega}_i \times {}^i r_i + {}^i\omega_i \times ({}^i\omega_i \times {}^i r_i))$	
Linear acceleration of the center of mass	
$\dot{v}_{ci} = \dot{v}_i + \dot{\omega}_i \times r_{ci} + \omega_i \times (\omega_i \times r_{ci})$	
${}^i \dot{v}_{ci} = {}^i \dot{v}_i + {}^i \dot{\omega}_i \times {}^i r_{ci} + {}^i \omega_i \times ({}^i \omega_i \times {}^i r_{ci})$	
Acceleration of gravity	
${}^i g = {}^iR_{i-1} {}^{i-1} g$	

The second step is the dynamic calculus of backward computation, as can be seen in Table 2. Note, only rotational joints are considered in both tables.

Table 2. Recursive newton-euler formulation. Backward dynamics.

Backward dynamics	
Inertial forces and moments	
$f_i^* = -m_i \dot{v}_{ci}$	
$n_i^* = -I_i \dot{\omega}_i - \omega_i \times (I_i \omega_i)$	
Force and torque balance equations about the center of mass	
$f_{i,i-1} = f_{i+1,i} - m_i g - f_i^*$	
$n_{i,i-1} = n_{i+1,i} + (r_i + r_{ci}) \times f_{i,i-1} - r_{ci} \times f_{i+1,i} - n_i^*$	
Torque in rotational joint	
$\tau_i = {}^{i-1}n_{i,i-1}^T {}^{i-1}z_{i-1}$	

The following assumptions have been made to simplify the equations of the Newton-Euler methodology:

- Mass and inertia of the gimbals are approximately zero or negligible.
- The center of mass of the Flywheel is aligned with the gimbal axis.
- Velocity and acceleration of the base body are not equal to zero.

The mass and inertia of the gimbal frame is neglected because the flywheel has the major contribution in the mass and inertia of the gyroscopes.

### 2.1. Data of the links

For the Newton-Euler approach, one gyroscope is composed of three links: base body, gimbal and flywheel. Each of these links is joined by a rotational joint, Fig. 3.

Before computing the forward kinematics and backward dynamics, each link must have a coordinate frame. Fig. 4 illustrates the frames and vectors defined for each link. A new frame,  $[\mathbf{x}_{0,i} \ \mathbf{y}_{0,i} \ \mathbf{z}_{0,i}]$ , is used to express the forces and moment exerted by the gyroscopes. This frame is fixed in the base body. The other two frames are  $[\mathbf{x}_{1,i} \ \mathbf{y}_{1,i} \ \mathbf{z}_{1,i}]$  and  $[\mathbf{x}_{2,i} \ \mathbf{y}_{2,i} \ \mathbf{z}_{2,i}]$ , with the former being the frame of the gimbals link and the latter being the frame of the flywheel link. These two frames are located at the same point, the center of the flywheel. The homogeneous matrix between the frames fixed in the base body,  $[\mathbf{x}_0 \ \mathbf{y}_0 \ \mathbf{z}_0]$  and  $[\mathbf{x}_{0,i} \ \mathbf{y}_{0,i} \ \mathbf{z}_{0,i}]$ , is,

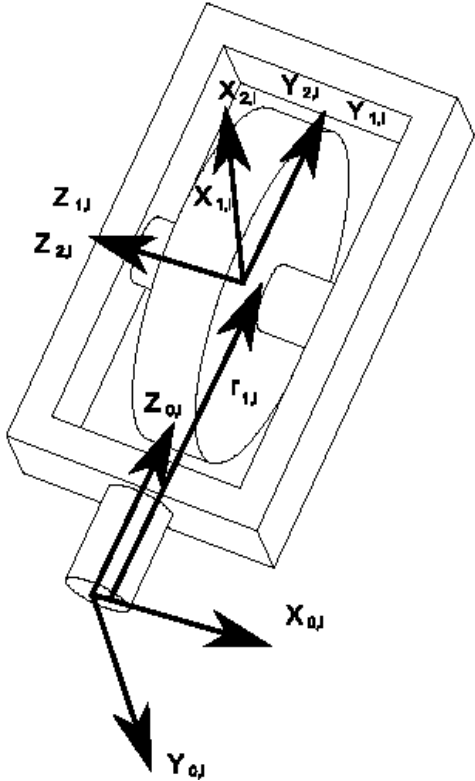


Figure 4. Frames used in the Newton-Euler algorithm.

$${}^b\mathbf{A}_{0,i} = \begin{bmatrix} ca_i & -sa_i c\beta & -sa_i s\beta & -sa_i r \\ sa_i & ca_i c\beta & ca_i s\beta & ca_i r \\ 0 & -s\beta & c\beta & 0 \\ 0 & 0 & 0 & 1 \end{bmatrix} \quad (1)$$

Where  $sa_i$ ,  $ca_i$ ,  $s\beta$ , and  $c\beta$  stands for  $\sin(a_i)$ ,  $\cos(a_i)$ ,  $\sin(\beta)$ , and  $\cos(\beta)$  respectively;  $r$  is the radius of the circle where the gyroscopes are located;  $a_i$  is the angle of the turn around axis  $\mathbf{z}_0$  to align  $\mathbf{y}_0$  with  $\mathbf{y}_i$ , and it has any of the values of  $\{0, \pi/2, \pi, 2\pi/3\}$  radians.

The Denavit-Hantenberg parameters for one gyroscope according to Fig. 4, are shown in Table 3. In this table  $L = \|\mathbf{r}_{1,i}\|$ , where  $\mathbf{r}_{1,i}$  is the vector from frame  $\{0, i\}$  to frame  $\{1, i\}$ .

Table 3.

Denavit - Hartenberg parameters.

Joint - i	$\alpha_i$	$a_i$	$d_i$	$\theta_i$
1	$\pi/2$	0	L	$\theta_1$ $-\pi/2$
2	0	0	0	$\theta_{1,2}$

1) Homogeneous Transformation Matrices: The DH transformation matrices for each link can be also computed, these are:

$${}^{0,i}\mathbf{A}_{1,i} = \begin{bmatrix} \sin(\theta_i) & 0 & -\cos(\theta_i) & 0 \\ -\cos(\theta_i) & 0 & -\sin(\theta_i) & 0 \\ 0 & 1 & 0 & L \\ 0 & 0 & 0 & 1 \end{bmatrix} \quad (2)$$

$${}^{1,i}\mathbf{A}_{2,i} = \begin{bmatrix} \cos(\theta_{i,2}) & -\sin(\theta_{i,2}) & 0 & 0 \\ \sin(\theta_{i,2}) & \cos(\theta_{i,2}) & 0 & 0 \\ 0 & 0 & 1 & 0 \\ 0 & 0 & 0 & 1 \end{bmatrix} \quad (3)$$

2) Position Vectors: The position of the frame  $\{1, i\}$  with respect to  $\{0, i\}$  is defined by vector  ${}^{0,i}\mathbf{r}_{c0,i}$ . The vector  ${}^{2,i}\mathbf{r}_{2,i}$  defines the position of  $\{2, i\}$  related to  $\{1, i\}$ . The mass centre of each link is defined by vectors  ${}^{0,i}\mathbf{r}_{c0,i}$  and  ${}^{1,i}\mathbf{r}_{c1,i}$ . These vectors have the following values,

$${}^{1,i}\mathbf{r}_{1,i} = [0 \ 0 \ L]^T \quad (4)$$

$${}^{2,i}\mathbf{r}_{2,i} = [0 \ 0 \ 0]^T \quad (5)$$

$${}^{0,i}\mathbf{r}_{c0,i} = [0 \ 0 \ 0]^T \quad (6)$$

$${}^{1,i}\mathbf{r}_{c1,i} = [0 \ 0 \ 0]^T \quad (7)$$

${}^{0,i}\mathbf{r}_{c0,i}$  is zero because the mass and inertia of the gimbals are neglected.

3) Inertia and mass for links: For both links the values of mass and inertia are,

$$m_{1,i} = 0 \quad (8)$$

$$m_{2,i} = m_2 \quad (9)$$

$${}^{1,i}\mathbf{I}_{1,i} = \mathbf{0} \quad (10)$$

$${}^{2,i}\mathbf{I}_{2,i} = \text{diag}([I_{xx} \ I_{yy} \ I_{zz}]) \quad (11)$$

4) Base Body conditions: Different to a typical robot, the base body of a 4-CMG is in motion, which allows it to have an angular and linear velocity as well as non-zero acceleration.

${}^{0,i}\boldsymbol{\omega}_{0,i}$ ,  ${}^{0,i}\dot{\boldsymbol{\omega}}_{0,i}$ ,  ${}^{0,i}\mathbf{v}_{0,i}$ ,  ${}^{0,i}\dot{\mathbf{v}}_{0,i}$ , not equal to zero.

## 2.2. Forward Kinematics

The following equations are derived after using the forward kinematics, table 1.

1) First link - gimbal axis: The first link has the following velocity and acceleration.

Angular Velocity

$$\boldsymbol{\omega}_{1,i} = \boldsymbol{\omega}_{0,i} + \mathbf{z}_{0,i}\dot{\theta}_i \quad (12)$$

Angular Acceleration

$$\dot{\boldsymbol{\omega}}_{1,i} = \dot{\boldsymbol{\omega}}_{0,i} + \mathbf{z}_{0,i}\ddot{\theta}_i + \boldsymbol{\omega}_{0,i} \times \mathbf{z}_{0,i}\dot{\theta}_i \quad (13)$$

Linear Velocity

$$\mathbf{v}_{1,i} = \mathbf{v}_{0,i} + \boldsymbol{\omega}_{0,i} \times \mathbf{r}_{1,i} \quad (14)$$

Because  $\mathbf{z}_{0,i}$  and  $\mathbf{r}_{1,i}$  are parallel.

Linear Acceleration

$$\dot{\mathbf{v}}_{1,i} = \dot{\mathbf{v}}_{0,i} + \dot{\boldsymbol{\omega}}_{0,i} \times \mathbf{r}_{1,i} + \boldsymbol{\omega}_{0,i} \times \dot{\boldsymbol{\omega}}_{0,i} \times \mathbf{r}_{1,i} \quad (15)$$

Acceleration of the center of mass

$$\dot{\mathbf{v}}_{c1,i} = \dot{\mathbf{v}}_{1,i} \quad (16)$$

2) Second Link - flywheel axis: Performing the same steps, as the first link, the results are,

Angular Velocity

$$\boldsymbol{\omega}_{2,i} = \boldsymbol{\omega}_{0,i} + \mathbf{z}_{0,i}\dot{\theta}_i + \mathbf{z}_{1,i}\dot{\theta}_{2,i} \quad (17)$$

Angular Acceleration

$$\dot{\boldsymbol{\omega}}_{2,i} = \dot{\boldsymbol{\omega}}_{0,i} + \mathbf{z}_{0,i}\ddot{\theta}_i + \boldsymbol{\omega}_{0,i} \times \mathbf{z}_{0,i}\dot{\theta}_i + \boldsymbol{\omega}_{0,i} \times \mathbf{z}_{1,i}\dot{\theta}_{2,i} + \dot{\theta}_i\dot{\theta}_{2,i}\mathbf{x}_{1,i} \quad (18)$$

Linear Velocity

$$\mathbf{v}_{2,i} = \mathbf{v}_{0,i} + \boldsymbol{\omega}_{0,i} \times \mathbf{r}_{1,i} \quad (19)$$

Linear Acceleration

$$\dot{\mathbf{v}}_{2,i} = \dot{\mathbf{v}}_{0,i} + \dot{\boldsymbol{\omega}}_{0,i} \times \mathbf{r}_{1,i} + \boldsymbol{\omega}_{0,i} \times \dot{\boldsymbol{\omega}}_{0,i} \times \mathbf{r}_{1,i} \quad (20)$$

Acceleration of the center of mass

$$\dot{\mathbf{v}}_{c2,i} = \dot{\mathbf{v}}_{2,i} \quad (21)$$

## 2.3. Backward Dynamics

The following dynamics equations for one gyroscope are obtained after applying the equations in table 2.

1) Second Body: By using backward dynamics, the torque required by the flywheel motor can be computed as the Inertial Forces and Moments

$$\mathbf{f}_{2,i}^* = -m_2\dot{\mathbf{v}}_{0,i} - m_2\dot{\boldsymbol{\omega}}_{0,i} \times \mathbf{r}_{1,i} - m_2\boldsymbol{\omega}_{0,i} \times \boldsymbol{\omega}_{0,i} \times \mathbf{r}_{1,i} \quad (22)$$

$$\mathbf{n}_{2,i}^* = -\mathbf{I}_{2,i}\dot{\boldsymbol{\omega}}_{0,i} - \boldsymbol{\omega}_{0,i} \times \mathbf{I}_{2,i}\boldsymbol{\omega}_{0,i} - \dot{\theta}_i I_{yy}\boldsymbol{\omega}_{0,i} \times \mathbf{y}_{1,i} - \dot{\theta}_{2,i} I_{zz}\boldsymbol{\omega}_{0,i} \times \mathbf{z}_{1,i} - \dot{\theta}_i I_{yy}\mathbf{y}_{1,i} - \dot{\theta}_i\dot{\theta}_{2,i} I_{zz}\mathbf{x}_{1,i} \quad (23)$$

Where the following relations were used,

$$\mathbf{I}_{2,i}\mathbf{z}_{0,i} = I_{yy}\mathbf{y}_{1,i} \quad (24)$$

$$\mathbf{I}_{2,i}\mathbf{z}_{1,i} = I_{zz}\mathbf{z}_{1,i} \quad (25)$$

$$\mathbf{I}_{2,i}\mathbf{x}_{1,i} = I_{xx}\mathbf{x}_{1,i} \quad (26)$$

Forces and Moments in the center of mass

$$\mathbf{f}_{21,i} = -m_2\mathbf{g} + m_2\dot{\mathbf{v}}_{0,i} + m_2\dot{\boldsymbol{\omega}}_{0,i} \times \mathbf{r}_{1,i} + m_2\boldsymbol{\omega}_{0,i} \times \boldsymbol{\omega}_{0,i} \times \mathbf{r}_{1,i} \quad (27)$$

$$\mathbf{n}_{2,i} = \mathbf{I}_{2,i}\dot{\boldsymbol{\omega}}_{0,i} + \boldsymbol{\omega}_{0,i} \times \mathbf{I}_{2,i}\boldsymbol{\omega}_{0,i} + \dot{\theta}_i I_{yy}\boldsymbol{\omega}_{0,i} \times \mathbf{y}_{1,i} + \dot{\theta}_{2,i} I_{zz}\boldsymbol{\omega}_{0,i} \times \mathbf{z}_{1,i} + \dot{\theta}_i I_{yy}\mathbf{y}_{1,i} + \dot{\theta}_i\dot{\theta}_{2,i} I_{zz}\mathbf{x}_{1,i} \quad (28)$$

Torque in joint

$$\boldsymbol{\tau}_{2,i} = \mathbf{z}_{1,i}^T \mathbf{I}_{2,i} \dot{\boldsymbol{\omega}}_{0,i} + \mathbf{z}_{1,i}^T \boldsymbol{\omega}_{0,i} \times \mathbf{I}_{2,i} \boldsymbol{\omega}_{0,i} + \dot{\theta}_i I_{yy} \mathbf{z}_{1,i}^T \boldsymbol{\omega}_{0,i} \times \mathbf{y}_{1,i} \quad (29)$$

2) First Body: In these steps the torque required by gimbal motor and the reaction moments and forces in the base body are computed. Inertial Forces and Moments

$$\mathbf{f}_1^* = 0 \quad (30)$$

$$\mathbf{n}_1^* = 0 \quad (31)$$

Forces and Moments in the center of mass

$$\mathbf{f}_{10,i} = -m_2\mathbf{g} + m_2\dot{\mathbf{v}}_{0,i} + m_2\dot{\boldsymbol{\omega}}_{0,i} \times \mathbf{r}_{1,i} + m_2\boldsymbol{\omega}_{0,i} \times \boldsymbol{\omega}_{0,i} \times \mathbf{r}_{1,i} \quad (32)$$

$$\mathbf{n}_{10,i} = \mathbf{I}_{2,i}\dot{\boldsymbol{\omega}}_{0,i} + \boldsymbol{\omega}_{0,i} \times \mathbf{I}_{2,i}\boldsymbol{\omega}_{0,i} + \dot{\theta}_i I_{yy}\boldsymbol{\omega}_{0,i} \times \mathbf{y}_{1,i} + \dot{\theta}_{2,i} I_{zz}\boldsymbol{\omega}_{0,i} \times \mathbf{z}_{1,i} + \dot{\theta}_i I_{yy}\mathbf{y}_{1,i} + \dot{\theta}_i\dot{\theta}_{2,i} I_{zz}\mathbf{x}_{1,i} - m_2\mathbf{r}_{1,i} \times \mathbf{g} + m_2\mathbf{r}_{1,i} \times \dot{\mathbf{v}}_{0,i} + m_2\mathbf{r}_{1,i} \times \dot{\boldsymbol{\omega}}_{0,i} \times \mathbf{r}_{1,i} + m_2\mathbf{r}_{1,i} \times \boldsymbol{\omega}_{0,i} \times \boldsymbol{\omega}_{0,i} \times \mathbf{r}_{1,i} \quad (33)$$

Torque in Joint

$$\boldsymbol{\tau}_{1,i} = \mathbf{z}_{0,i}^T \mathbf{I}_{2,i} \dot{\boldsymbol{\omega}}_{0,i} + \mathbf{z}_{0,i}^T \boldsymbol{\omega}_{0,i} \times \mathbf{I}_{2,i} \boldsymbol{\omega}_{0,i} + \dot{\theta}_2 I_{zz} \mathbf{z}_{0,i}^T \boldsymbol{\omega}_{0,i} \times \mathbf{z}_{1,i} + \dot{\theta}_i I_{yy} \quad (34)$$

#### 2.4. Dynamic Equation for Base Body

The total force and moment exerted on the base body, is the sum of the force and torque for each gyroscope's equation, (32) and (33).

$$\mathbf{F}_{ext} + m_0 \mathbf{g} = m_0 \dot{\mathbf{v}}_b + \sum_{i=1}^4 \mathbf{f}_{10,i} \quad (35)$$

$$\boldsymbol{\tau}_{ext} = \mathbf{I}_b \dot{\boldsymbol{\omega}}_b + \boldsymbol{\omega}_b \times \mathbf{I}_b \boldsymbol{\omega}_b + \sum_{i=1}^4 (\mathbf{n}_{10,i} + \mathbf{r}_i \times \mathbf{f}_{10,i}) \quad (36)$$

If  $\mathbf{r}_i$ ,  $\mathbf{v}_{0,i}$ ,  $\dot{\mathbf{v}}_{0,i}$ ,  $\boldsymbol{\omega}_{0,i}$  and  $\dot{\boldsymbol{\omega}}_{0,i}$  are defined by the following expressions,

$$\mathbf{r}_1 = [0, r, 0]^T \quad (37)$$

$$\mathbf{r}_2 = [-r, 0, 0]^T \quad (38)$$

$$\mathbf{r}_3 = [0, -r, 0]^T \quad (39)$$

$$\mathbf{r}_4 = [r, 0, 0]^T \quad (40)$$

$$\boldsymbol{\omega}_0 = \boldsymbol{\omega}_b \quad (41)$$

$$\dot{\boldsymbol{\omega}}_0 = \dot{\boldsymbol{\omega}}_b \quad (42)$$

$$\mathbf{v}_{0,i} = \mathbf{v}_b + \boldsymbol{\omega}_b \times \mathbf{r}_i \quad (43)$$

$$\dot{\mathbf{v}}_{0,i} = \dot{\mathbf{v}}_b + \dot{\boldsymbol{\omega}}_b \times \mathbf{r}_i + \boldsymbol{\omega}_b \times \boldsymbol{\omega}_b \times \mathbf{r}_i \quad (44)$$

Then eq. (32)-(33) are expressed in terms of base body variables,

$$\begin{aligned} \mathbf{f}_{10,i} = & -m_2 \mathbf{g} + m_2 \dot{\mathbf{v}}_b + m_2 \dot{\boldsymbol{\omega}}_b \times \mathbf{r}_i \\ & + m_2 \boldsymbol{\omega}_b \times \boldsymbol{\omega}_b \times \mathbf{r}_i + m_2 \dot{\boldsymbol{\omega}}_b \times \mathbf{r}_{1,i} \\ & + m_2 \boldsymbol{\omega}_b \times \boldsymbol{\omega}_b \times \mathbf{r}_{1,i} \end{aligned} \quad (45)$$

$$\begin{aligned} \mathbf{n}_{10,i} = & \mathbf{I}_{2,i} \dot{\boldsymbol{\omega}}_b + \boldsymbol{\omega}_b \times \mathbf{I}_{2,i} \boldsymbol{\omega}_b + \dot{\theta}_i I_{yy} \boldsymbol{\omega}_b \times \mathbf{y}_{1,i} \\ & + \dot{\theta}_{2,i} I_{zz} \boldsymbol{\omega}_b \times \mathbf{z}_{1,i} + \ddot{\theta}_i I_{yy} \mathbf{y}_{1,i} \\ & + \dot{\theta}_i \dot{\theta}_{2,i} I_{zz} \mathbf{x}_{1,i} - m_2 \mathbf{r}_{1,i} \times \mathbf{g} \\ & + m_2 \mathbf{r}_{1,i} \times \dot{\mathbf{v}}_b + m_2 \mathbf{r}_{1,i} \times \dot{\boldsymbol{\omega}}_b \times \mathbf{r}_i \\ & + m_2 \mathbf{r}_{1,i} \times \boldsymbol{\omega}_b \times \boldsymbol{\omega}_b \times \mathbf{r}_i \\ & + m_2 \mathbf{r}_{1,i} \times \dot{\boldsymbol{\omega}}_b \times \mathbf{r}_{1,i} \\ & + m_2 \mathbf{r}_{1,i} \times \boldsymbol{\omega}_b \times \boldsymbol{\omega}_b \times \mathbf{r}_{1,i} \end{aligned} \quad (46)$$

The equation of forces is obtained after replacing (45) in (35). This preliminary result is simplified if the relationship for  $\mathbf{r}_i$  is used in conjunction with the fact that for a symmetrical 4-CMG the vectors  $\mathbf{r}_{1,i}$  are,

$$\mathbf{r}_{1,0} = -\mathbf{r}_{1,2} \quad (47)$$

$$\mathbf{r}_{1,1} = -\mathbf{r}_{1,3} \quad (48)$$

The final equation is,

$$\mathbf{F}_{ext} = (m_0 + 4m_2) \dot{\mathbf{v}}_b - (m_0 + 4m_2) \mathbf{g} \quad (49)$$

Before computing the dynamic equation for moments, the expression  $\mathbf{n}_{10,i} + \mathbf{r}_i \times \mathbf{f}_{10,i}$  is simplified by using the following relations,

$$\mathbf{r}'_i = \mathbf{r}_i + \mathbf{r}_{1,i} \quad (50)$$

$$\sum_{i=0}^4 m_2 \mathbf{r}'_i \times \mathbf{g} = 0 \quad (51)$$

$$\sum_{i=0}^4 m_2 \mathbf{r}'_i \times \dot{\mathbf{v}}_b = 0 \quad (52)$$

$$\mathbf{a} \times \mathbf{b} \times \mathbf{b} \times \mathbf{a} = -\mathbf{b} \times \mathbf{a} \times \mathbf{a} \times \mathbf{b} \quad (53)$$

The obtained result is,

$$\begin{aligned} & \sum_{i=0}^4 (\mathbf{n}_{10,i} + \mathbf{r}_i \times \mathbf{f}_{10,i}) \\ & = \sum_{i=0}^4 (\mathbf{I}_{2,i} \dot{\boldsymbol{\omega}}_b - m_2 \mathbf{r}'_i \times \mathbf{r}'_i \times \dot{\boldsymbol{\omega}}_b \\ & + \boldsymbol{\omega}_b \times \mathbf{I}_{2,i} \boldsymbol{\omega}_b - m_2 \boldsymbol{\omega}_b \times \mathbf{r}'_i \times \mathbf{r}'_i \\ & \times \boldsymbol{\omega}_b + \dot{\theta}_i I_{yy} \boldsymbol{\omega}_b \times \mathbf{y}_{1,i} + \dot{\theta}_{2,i} I_{zz} \boldsymbol{\omega}_b \\ & \times \mathbf{z}_{1,i} + \dot{\theta}_i I_{yy} \mathbf{y}_{1,i} + \dot{\theta}_i \dot{\theta}_{2,i} I_{zz} \mathbf{x}_{1,i}) \end{aligned} \quad (54)$$

It is a common practice to represent the torque's equation in the base body coordinate frame. In this frame, the following matrices are defined,

$${}^b \mathbf{X}_1 = [{}^b x_{1,1} \quad \dots \quad {}^b x_{1,4}] \quad (55)$$

$${}^b \mathbf{Y}_1 = [{}^b y_{1,1} \quad \dots \quad {}^b y_{1,4}] \quad (56)$$

$$\dot{\boldsymbol{\theta}} = [\dot{\theta}_1 \quad \dots \quad \dot{\theta}_4]^T \quad (57)$$

$$\ddot{\boldsymbol{\theta}} = [\ddot{\theta}_1 \quad \dots \quad \ddot{\theta}_4]^T \quad (58)$$

$${}^b \mathbf{I}_t = {}^b \mathbf{I}_b + \sum_{i=0}^4 ({}^b \mathbf{R}_i {}^i \mathbf{I}_i {}^b \mathbf{R}_i^T - m_2 {}^b \tilde{\mathbf{r}}'_i {}^b \tilde{\mathbf{r}}'_i) \quad (59)$$

$${}^b \mathbf{D}_i = \sum_{i=0}^4 ({}^b \mathbf{R}_i {}^i \mathbf{I}_i {}^b \mathbf{R}_i^T - m_2 {}^b \tilde{\mathbf{r}}'_i {}^b \tilde{\mathbf{r}}'_i) \quad (60)$$

$${}^b \mathbf{I}_t = {}^b \mathbf{I}_b + {}^b \mathbf{D}_i \quad (61)$$

Where  $\tilde{\mathbf{a}}$  is the matrix equivalent of the cross product,  $\mathbf{a} \times$

$$\tilde{\mathbf{a}} = \begin{bmatrix} 0 & -a_3 & a_2 \\ a_3 & 0 & -a_1 \\ -a_2 & a_1 & 0 \end{bmatrix} \quad (62)$$

Therefore, the torque equation over the base body is then expressed as,

$$\begin{aligned} {}^b \boldsymbol{\tau}_{ext} = & {}^b \mathbf{I}_b \dot{\boldsymbol{\omega}}_b + {}^b \tilde{\boldsymbol{\omega}}_b {}^b \mathbf{I}_b \boldsymbol{\omega}_b + I_{yy} {}^b \mathbf{Y}_1 \ddot{\boldsymbol{\theta}} \\ & + \dot{\theta}_{2,zz} {}^b \mathbf{X}_1 \dot{\boldsymbol{\theta}} + I_{yy} {}^b \tilde{\boldsymbol{\omega}}_b {}^b \mathbf{Y}_1 \dot{\boldsymbol{\theta}} \\ & + \dot{\theta}_{2,zz} I_{zz} {}^b \tilde{\boldsymbol{\omega}}_b \sum_{i=1}^4 {}^b \mathbf{z}_{1,i} \end{aligned} \quad (63)$$

Where  ${}^b \mathbf{X}_1$ ,  ${}^b \mathbf{Y}_1$ ,  ${}^b \mathbf{z}_{1,i}$  and  ${}^b \mathbf{R}_i$  are,

$${}^b \mathbf{X}_1 = \begin{bmatrix} s\theta_1 & c\beta c\theta_2 & -s\theta_3 & -c\beta c\theta_4 \\ -c\beta c\theta_1 & s\theta_2 & c\beta c\theta_3 & -s\theta_4 \\ s\beta c\theta_1 & s\beta c\theta_2 & s\beta c\theta_3 & s\beta c\theta_4 \end{bmatrix} \quad (64)$$

$${}^b \mathbf{Y}_1 = \begin{bmatrix} 0 & -s\beta & 0 & s\beta \\ s\beta & 0 & -s\beta & 0 \\ c\beta & c\beta & c\beta & c\beta \end{bmatrix} \quad (65)$$

$${}^b \mathbf{z}_{1,1} = [-c\theta_1 \quad c\beta s\theta_1 \quad s\beta s\theta_1]^T \quad (66)$$

$${}^b \mathbf{z}_{1,2} = [c\beta s\theta_2 \quad c\theta_2 \quad s\beta s\theta_2]^T \quad (67)$$

$${}^b\mathbf{z}_{1,3} = [c\theta_3 \quad c\beta s\theta_3 \quad s\beta s\theta_3]^T \quad (68)$$

$${}^b\mathbf{z}_{1,4} = [c\beta s\theta_4 \quad -c\theta_4 \quad s\beta s\theta_4]^T \quad (69)$$

$${}^b\mathbf{R}_1 = \begin{bmatrix} s\theta_1 & 0 & -c\theta_1 \\ -c\beta c\theta_1 & s\beta & -c\beta s\theta_1 \\ s\beta c\theta_1 & c\beta & s\beta s\theta_1 \end{bmatrix} \quad (70)$$

$${}^b\mathbf{R}_2 = \begin{bmatrix} c\beta s\theta_2 & -s\beta & c\beta s\theta_2 \\ s\theta_2 & 0 & c\theta_2 \\ s\beta c\theta_2 & c\beta & s\beta s\theta_2 \end{bmatrix} \quad (71)$$

$${}^b\mathbf{R}_3 = \begin{bmatrix} -s\theta_3 & 0 & c\theta_3 \\ c\beta c\theta_3 & -s\beta & c\beta s\theta_3 \\ s\beta c\theta_3 & c\beta & s\beta s\theta_3 \end{bmatrix} \quad (71)$$

$${}^b\mathbf{R}_4 = \begin{bmatrix} -c\beta s\theta_4 & s\beta & -c\beta s\theta_4 \\ -s\theta_4 & 0 & -c\theta_4 \\ s\beta c\theta_4 & c\beta & s\beta s\theta_4 \end{bmatrix} \quad (71)$$

Finally, the torque eq. (34) and (29), can be rearranged and expressed in base body coordinates as,

$$\begin{aligned} \boldsymbol{\tau}_{2,i} = & {}^b\mathbf{z}_{1,i}^T {}^b\mathbf{R}_i {}^i\mathbf{I}_i {}^b\mathbf{R}_i^T {}^b\dot{\boldsymbol{\omega}}_b \\ & + {}^b\mathbf{z}_{1,i}^T {}^b\tilde{\boldsymbol{\omega}}_b {}^b\mathbf{R}_i {}^i\mathbf{I}_i {}^b\mathbf{R}_i^T {}^b\boldsymbol{\omega}_b \\ & + \dot{\theta}_i I_{yy} {}^b\mathbf{z}_{1,i}^T {}^b\tilde{\boldsymbol{\omega}}_b {}^b\mathbf{y}_{1,i} \end{aligned} \quad (74)$$

$$\begin{aligned} \boldsymbol{\tau}_{1,i} = & {}^b\mathbf{y}_{1,i}^T {}^b\mathbf{R}_i {}^i\mathbf{I}_i {}^b\mathbf{R}_i^T {}^b\dot{\boldsymbol{\omega}}_b \\ & + {}^b\mathbf{y}_{1,i}^T {}^b\tilde{\boldsymbol{\omega}}_b {}^b\mathbf{R}_i {}^i\mathbf{I}_i {}^b\mathbf{R}_i^T {}^b\boldsymbol{\omega}_b \\ & + \theta_{2,i} I_{zz} {}^b\mathbf{y}_{1,i}^T {}^b\tilde{\boldsymbol{\omega}}_b {}^b\mathbf{z}_{1,i} + \dot{\theta}_i I_{yy} \end{aligned} \quad (75)$$

These equations are useful to select the motors for each actuated joint [13].

### 3. Numerical example

The eq. (74) and (75) are useful for computing the motor requirements, while equation (63) is used to create a steering control law for the 4-CMG as is done in [14]. In the case of a flywheel motor, eq. (74), only the last term is traditionally taken into account to compute the required torque, but a numerical simulation can show how the proposed equations are better than the traditional approach.

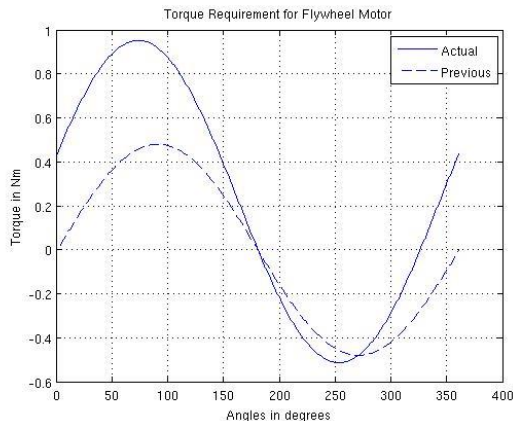


Figure 5. Effect of body motion in flywheel torque.

Let us assume a flywheel with inertia of 0.16 in x and y axis and a value of 0.308 in z axis, which is rotating at a speed of 10000 rpm. If the body has an angular velocity and acceleration, it is clear in eq. (74) than the first two terms contribute to the total torque. Fig. 5 illustrates the results obtained for a unit angular velocity and acceleration. The continuous line represents the torque computed with eq. (74), while the dotted line is the torque computed using the traditional approach.

### 4. CONCLUSIONS

A new dynamic model for a 4-CMG was derived using the Newton-Euler algorithm, a methodology commonly used in Robotics. Although some simplifications were done, the dynamic model is useful to study the behavior of a 4-CMG. The obtained dynamic model can also be used for computing a control law for a 4-CMG. Torque equations for the rotational joints were also found. A simulation was performed to illustrate the benefit of the proposed equations. These equations are also useful to compute and help in selecting the proper motors that will drive the joints.

### References

- [1] Kuhns, M. and Rodriguez, A. Singularity avoidance control laws for a multiple CMG spacecraft attitude control system, Proceedings of the American Control Conference (ACC), pp. 2892–2893, 1994.
- [2] Kuhns, M. and Rodriguez, A. A preferred trajectory tracking steering law for spacecraft with redundant CMGs, Proceedings of the American Control Conference (ACC), pp. 3111–3115, 1995.
- [3] Oh, S. and Vadali, S. R. Feedback control and steering laws for spacecraft using single gimbal control moment gyros, *Astronautical Sciences*, 39 (2), pp. 183–203, 1991.
- [4] Thornton, B., Ura, T., Nose, Y. and Turnock, S. Internal actuation of underwater robots using control moment gyros, *Proceedings of Oceans*, pp. 591–598, 2005.
- [5] Thornton, B., Ura, T. and Nose, Y. Wind-up AUVs: Combined energy storage and attitude control using control moment gyros. *Proceedings of Oceans*, pp. 1-9, 2007
- [6] Lappas, V. J., Steyn, W. H. and Underwood, C. I. Torque amplification of control moment gyros, *IEEE Electronics Letters*, 38 (15), pp. 837–839, 2002.
- [7] Tekinalp, O., Elmas, T. and Yavrucuk, I. Gimbal angle restricted control moment gyroscope clusters, *Proceedings of 4th International Conference on Recent Advances in Space Technologies (RAST)*, pp. 585-590, 2009.
- [8] Ford, K. A. and Hall, C. D. Singular direction avoidance steering for control-moment gyros, *Journal Guidance Control and Dynamics*, 23 (4), pp. 648–656, 2000.
- [9] Bedrossian, N. S., Paradiso, J., Bergmann, E. V. and Rowell, D. Redundant single gimbal control moment gyroscope singularity analysis, *Journal Guidance Control and Dynamics*, 13 (6), pp. 1096–1101, 1990.
- [10] Toz, M. and Kucuk, S. A comparative study for computational cost of fundamental robot manipulators, *Proceedings of International Conference on Industrial Technology (ICIT)*, pp. 289-293, 2011.
- [11] Negrean, I., Schonstein, C., Negrean, D.C., Negrean, A.S. and Duca, A.V. Formulations in robotics based on variational principles, *Proceeding of International Conference on Automation Quality and Testing Robotics (AQTR)*, pp. 1-6, 2010.

[12] Tsai, L. W. Robot Analysis: The Mechanics of Serial and Parallel Manipulators. Jon Wiley & Sons, Inc., 1999.

[13] Jaramillo, A. Franco, E. Guasch, L. Estimación de parámetros invariantes para un motor de inducción. Dyna, 78 (169), pp. 88–94, 2011.

[14] Yime, E., Quintero, J., Saltaren R. and Aracil R. A new Approach for Avoiding Internal Singularities in CMG with Pyramidal Shape Using Sliding Control. Proceedings of European Control Conference (ECC), pp. 125-132, 2009.

**E. Yime-Rodríguez** is a Mechanical Engineer, graduated from Universidad del Norte, with a PhD in robotics, from Universidad Politecnica de Madrid, who actually work for Universidad Tecnologica de Bolivar, located in Cartagena, Colombia. His major research areas are parallel and serial robotics, with emphasis in kinematics, dynamics and nonlinear control. Recently he has gained significant experience in mechanical and mechatronics design applied to robotics. He can be contacted to eyime@unitecnologica.edu.co

**C. A. Peña-Cortés** has been a Professor at Universidad de Pamplona in the Department of Mechatronics, Mechanics and Industrial Engineering since 2004. He received the Electromechanic Engineering degree in 2001 from Universidad Pedagógica y Tecnológica de Colombia, an MSc Degree in Electronics and Computers Engineering in 2003 from Universidad de los Andes, and his PhD degree in Automatics and Robotics from Universidad Politécnica de Madrid in 2009. His researches are focused on Service Robots, Telerobotics and Parallel Robots.

**W. M. Rojas-Contreras** is full professor of the Pamplona University. He became a systems engineer in Francisco de Paula Santander University. He received specialist degree from Industrial University of Santander. He obtained a master degree in computer science from Autonomous University. He is candidate to PhD in Applied Sciences from Andes University. Now, he is Dean of Engineering and Architecture Faculty and head of Computer Science research Group. His researches are focused on software engineering and project management software.